Carbon-Dot and Quantum-Dot-Coated Dual-Emission Core-Satellite Silica Nanoparticles for Ratiometric Intracellular...

Article *in* Analytical Chemistry · June 2016

DOI: 10.1021/acs.analchem.6b01941

CITATIONS
10

READS
79

8 authors, including:

Long Wu
Huazhong Agricultural University
19 PUBLICATIONS **77** CITATIONS
SEE PROFILE

Zhicheng Lu
Huazhong Agricultural University
28 PUBLICATIONS **375** CITATIONS
SEE PROFILE

Hagar Shendy El-Tokhy
Benha University, Faculty of Agriculture
2 PUBLICATIONS **10** CITATIONS
SEE PROFILE

He-You Han
Huazhong Agricultural University
165 PUBLICATIONS **2,642** CITATIONS
SEE PROFILE

analytical chemistry

Article

pubs.acs.org/ac

Carbon-Dot and Quantum-Dot-Coated Dual-Emission Core–Satellite Silica Nanoparticles for Ratiometric Intracellular Cu^{2+} Imaging

Chenchen Zou,[†] Mohamed Frahat Foda,[†] Xuecai Tan,[‡] Kang Shao,[†] Long Wu,[†] Zhicheng Lu,[†] Hagar Shendy Bahlol,[†] and Heyou Han*[,†]

[†]State Key Laboratory of Agricultural Microbiology, College of Science, Huazhong Agricultural University, Wuhan 430070, P. R. China

[‡]School of Chemistry and Chemical Engineering, Guangxi University for Nationalities, Nanning 530008, P. R. China

Supporting Information

ABSTRACT: Copper (Cu^{2+}) is physiologically essential, but excessive Cu^{2+} may cause potential risk to plants and animals due to the bioaccumulative properties. Hence, sensitive recognition is crucial to avoid overintake of Cu^{2+}, and visual recognition is more favored for practical application. In this work, a dual-emission ratiometric fluorescent nanoprobe was developed possessing the required intensity ratio, which can facilitate the sensitive identification of Cu^{2+} by the naked eye. The probe hybridizes two fluorescence nanodots (quantum dots (QDs) and carbon dots (CDs)). Although both of them can be viable fluorescence probes for metal ion detection, rarely research has coupled this two different kinds of fluorescence material in one nanosensor to fabricate a selectively ratiometric fluorescence probe for intracellular imaging. The red emitting CdTe/CdS QDs were capped around the silica microsphere to serve as the response signal label, and the blue-emitting CDs, which is insensitive to the analyte, were covalently attached to the QDs surface to act as the reference signal. This core–satellite hybrid sphere not only improves the stability and brightness of QDs significantly but also decreases the cytotoxicity toward HeLa cells tremendously. Moreover, the Cu^{2+} could quench the QDs emission effectively but have no ability for reduction of the CDs emission. Accordingly, a simple, efficient, and precise method for tracing Cu^{2+} was proposed. The increase of Cu^{2+} concentration in the series of $0–3 \times 10^{-6}$ M was in accordance with linearly decrease of the F_{650}/F_{425} ratio. As for practical application, this nanosensor was utilized to the ratiometric fluorescence imaging of copper ions in HeLa cells.

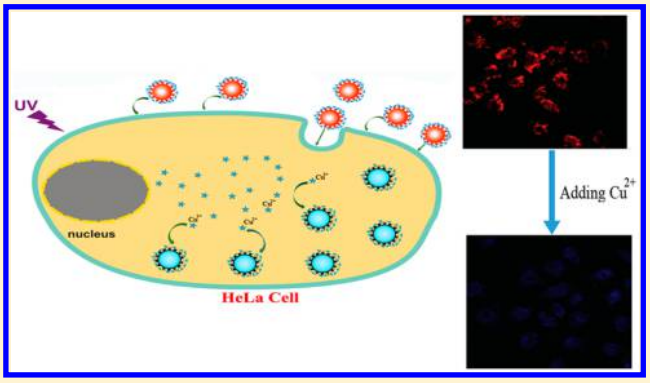

Currently, environmental pollution caused by heavy metals has become a severe problem due to the indestructibility of these metals in addition to their toxic effects on living organisms.[1] Copper, which is one of the most vital transition metals to the human body, is physiologically essential in several aspects, such as bone formation, cellular respiration, and connective tissue development, and serves as a significant catalytic cofactor for various metallo-enzymes.[2] However, an excessive amount of copper may exhibit high toxicity and may cause severe damage to the central nervous system, resulting in disorders associated with neurodegenerative diseases (e.g., Wilson's and Alzheimer's diseases).[3,4] According to the guidelines for drinking-water quality of the World Health Organization (WHO), copper is identified as a "significant chemical element for health in drinking water." The recommended daily allowance of copper suggested by National Research Council ranges from 1.5 to 3.0 mg for adults, 1.5 to 2.5 mg for children, and 0.4 to 0.6 mg for infants.[5,6] Thus, the identification and measurement of copper ions (Cu^{2+}) in the environmental matrix and biological fluids have become increasingly important.

During the past 2 decades, a large number of fluorescent probes have been developed for detecting different kinds of metal ions based on the quenching mechanism or target-triggered fluorescent enhancement.[7,8] However, the probes based on signal emission intensity changes are likely to be influenced by some factors, such as instrumental efficiency, environmental conditions, and the concentration of probe molecules. The ratiometric fluorescent probe signal discrepancy is easier to be distinguished by the naked eye, paralleled with the fluorescence quenching probe signal. More interestingly, the ratiometric fluorescent probe offers a built-in environmental interference correction as mentioned above, which excludes the fluctuation of light excitation intensity.[9−14] In recent years, dual-emission fluorescent nanoparticles (NPs) have attracted substantial research interest.[15−23] For instance, Yao et al. designed a dual-emission ratiometric fluorescence probe by embedding the red-emitting quantum dots (QDs) in silica NPs

Received: May 18, 2016
Accepted: June 27, 2016
Published: June 27, 2016

DOI: 10.1021/acs.analchem.6b01941
Anal. Chem. 2016, 88, 7395−7403

Scheme 1. Ratiometric Nanoprobe Structure Schematic Illustration and the Visual Recognition Principle for Cu^{2+}

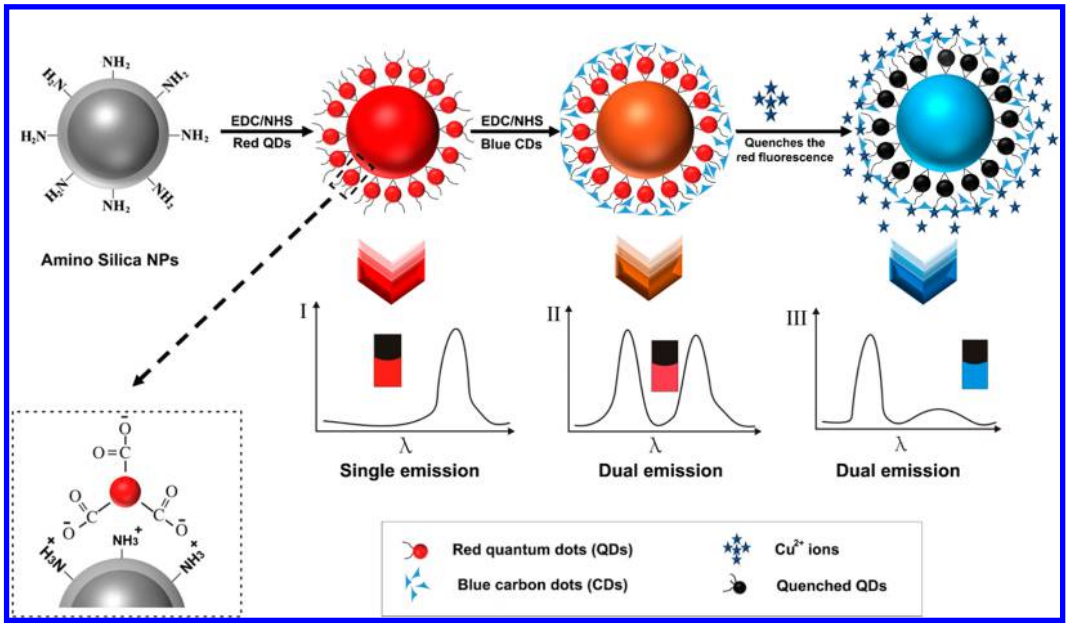

to serve as a reference signal and subsequently covalently linking the green-emitting QDs onto the surface to be sensitively quenched by the analyte.[24] This probe was developed to detect the Cu^{2+} in both lake and mineral water samples, mainly to monitor the Cu^{2+} residues on herb leaves. In Yan's work,[25] a sensitive sensor was used for detecting organophosphorus pesticides by coupling two contrarily colored CdTe QDs: the red light emission QDs were embedded in the silica microsphere to serve as a signal reference source, and the blue light emission QDs were covalently coated on the surface of the silica microsphere as a signal response source which could be quenched by AuNPs based on IFE (the inner-filter effect). However, the fluorescence could be turned on by the electrostatic attraction between protamine and AuNPs. Similarly, in Sun's work,[26] the blue light emission graphene quantum dots and the yellow light emission CdTe QDs were used as an internal standard and a response signal, respectively. This photoluminescence probe exhibited selective sensing for monitoring intracellular Cu^{2+}. Hereby, on the basis of these related reports, we found out that the way of entrapping the reference signal labels into the silica microsphere will tremendously reduce the intensity of quantum dots; Moreover, the fewer differences of the strong emission peak wavelength between the response and reference signal labels cannot avoid the interloping among the two emission peaks, and it is not favorable for the ratiometric fluorescence nanoprobe in the visual recognition of metal ions; however, not all of the ratiometric fluorescence probes are biocompatible enough to be applied in intracellular imaging. In that case, we chose two typical nanodots (carbon dots (CDs) and QDs) to fabricate a nontoxic dual-emission ratiometric fluorescence probe.

CDs have attracted much interest because of their low cytotoxicity, good water solubility, chemical inertness, easy preparation, high photoluminescence,[27,28] and excellent biocompatibility.[29,30] Besides, QDs have exceptional optical properties, such as size-dependent emission, narrow emission spectra, and continuous excitation spectra.[31−34] Both CDs and QDs are highly sensitive ion sensor to be applied in biology, pharmacology, and environmental science due to the highly sensitive response of ions to their surface states. Herein, a ratiometric fluorescence probe which can sensitively identify copper ions was designed. Compared with the traditional method, our probe shows higher sensitivity for ion detection and improved biocompatibility. Specifically, we integrated the CdTe/CdS QDs and CDs to fabricate a novel core−satellite hybrid nanosphere, in which the fluorescence of red emissive QDs is sensitively quenched by the analyte, whereas the outermost layer (CDs) is insensitive to the analyte. In this core−satellite ratiometric fluorescence probe, we used silica microspheres as a carrier loaded with an enormous number of quantum dots as signal labels on the surface which can enhance the brightness and stability of the fluorescence signal. Meanwhile, the outer-most layer of carbon dots densely packed around the SiO_2@QDs nanomicrospheres played an intensive protection role that can tremendously reduce the toxicity of the nanosensor, resulting in improving the biocompatibility of the probe, which was further confirmed by the MTT assay and the ratiometric fluorescence imaging of Cu^{2+} in HeLa cells. Additionally, the outermost layer (CDs) provided inherent correction for environmental defects and eliminated the variability of both probe concentration and excitation light intensity.

Notably, the MPA-capped CdTe/CdS QDs presented good sensitivity for the visual recognition of copper ions (Cu^{2+}) in aqueous solution.[35−39] The fluorescence emission of QDs has been proposed to be a consequence of the radiative recombination of the trapped electrons and holes on the surface,[40] and the quench of the fluorescence of the QDs is due to the highly sensitive response to copper ions to their surface states. Whereas, the CDs-APTES as a perfect fluorescence reference does not have the ability to recognize Cu^{2+},[30,41] and the amino groups on the CDs are covalently conjugated with the carboxyl groups on the MPA-capped CdTe QDs via a carbodiimide-mediated approach. Herein, we reveal the usage of QDs as a response signal report unit for the assembly of an efficient ratiometric fluorescence nanoprobe, which shows high

DOI: 10.1021/acs.analchem.6b01941
Anal. Chem. 2016, 88, 7395−7403

selectivity and sensitivity for the visual recognition of copper ions (Cu^{2+}) in aqueous solution and cell imaging (Scheme 1).

EXPERIMENTAL SECTION

Reagents. The initial materials needed in the synthesis of CdTe/CdS QDs were used without any additional purification. $CdCl_2·2.5H_2O$ (99.0%), $NaBH_4$ (96.0%), and tellurium powder (99.9%) were received from Sinopharm Chemical Regent Co. Ltd. (Shanghai, China). Sodium silicate solution (SiO_2, wt 27%), Tetraethoxysilane (TEOS), mercaptopropionic acid (MPA,99%), (3-aminopropyl) triethoxysilane (APTS), 3-(4,5-dimethylthiazol-2-yl)-2,5-diphenyl tetrazolium bromide (MTT), and dimethyl sulfoxide (DMSO) were purchased from Sigma-Aldrich Chemicals Co. Glycerin, ethanol, copper chloride ($CuCl_2$), and commonly used solvents and salts were obtained from Shanghai Chemical. Throughout the entire experimental stages, high-purity ultrapure water from a Millipore (18.2 MΩ cm) system was intended for all aqueous solution.

Apparatus. A Zeiss 510 META confocal laser scanning microscope was applied for fluorescence measurement. VG Multilab 2000 X-ray photoelectron spectrometer was used for measuring X-ray photoelectron spectroscopy (XPS) data. An FEI Tecnai G20 transmission electron microscope (FEI) operating at an acceleration voltage of 200 kV was utilized for high-resolution transmission electron microscopy (HRTEM) images. A JEM-2010 transmission electron microscope (JEOL, Japan) was used to collect the transmission electron microscopy (TEM) images. Hydrodynamic diameters were measured by using dynamic light scattering (DLS) technique on Malvern Zetasizer Nanoseries (Malvern, England) with 633 nm laser excitation at 25 °C.

Synthesis of CDs. The CDs we used were produced by a green hydrothermal synthesis method according to a previously reported method with some modifications.[30] Briefly, 1.0 mL of (3-aminopropyl) triethoxysilane (APTS) which contained multiple amino groups mixed with 9.0 mL of glycerol was loaded in a tetrafluoroethylene pot and heated to 200 °C under argon flow gas. The reaction was stopped after 30 min, and the mixture was allowed to cool down to room temperature. Then, the yellow product was subjected to dialysis in a dialysis bag (retained molecular weight, 1000 Da); the obtained CDs-APTES were highly dispersible in water. The focal value of this method is that both carbonization and surface amino-functionalization can proceed simultaneously all through the reaction to produce liberal primary amino groups on the surface of CDs, which is promising for the subsequent covalent conjugation.

Preparation of Amino-Silica NPs Loaded with Red CdTe/CdS QDs. MPA-capped CdTe/CdS $core_{small}/shell_{thick}$ QDs were synthesized following the previously described method.[42−46] Monodispersed silica nanospheres were synthesized consistent with the previously reported procedure with some modifications.[47,48] The obtained silica nanosphere solution was centrifuged to remove extra reactant, and the precipitate was redissolved in ethanol. To produce a self-assembled amino-terminated monolayer, hydroxyl groups on the surface of silica microspheres were coupled with APTS. A volume of 2.0 mL of silica NPs were redispersed in the prepared APTS solution obtaining 10% concentration, followed by stirring for 2 h at room temperature. The amino-functionalized silica NPs were obtained by centrifugation and cleaned three times with ethanol and water, respectively. Before the QDs were loaded onto the silica NPs, EDC was applied to activate the carboxylic groups on MPA-capped QDs. Then the unbound QDs were removed by continuous centrifugation and washing with water three times. Finally, the as-prepared QDs-loaded silica NPs were redispersed in water to a final volume of 2.0 mL.

Fabrication of CDs-Coated and QDs-Loaded Dual-Emission Silica NPs. A total volume of 2.0 mL of the presynthesis QDs-loaded silica NPs was dissolved in 2.0 mL of EDC (20 mg/mL). After that, 1.0 mL of CDs was added and kept stirring at room temperature. Soon afterward, the reaction combination was centrifuged and the achieved dual-emission silica NPs were cleaned three times with ultrapure water and then redispersed in water to a final volume of 2.0 mL for additional application. The supernatant was found to be clear (no color was observed), and the fluorescence of the redispersed silica NPs showed no noticeable changes, representing that the unbound QDs and CDs on the acquired dual-emission silica NPs had been carefully removed.

Detection of Cu^{2+} Ions. All the fluorescence detection was accomplished in phosphate buffer solution (PB, 10 mM, pH = 7.4). A volume of 1 mL of the above dual-emission silica NPs was centrifuged and redispersed into 6 mL of PB solution for further analysis. The stock solution of Cu^{2+} was prepared by dissolving an appropriate amount of $CuCl_2$ in water. The detection was conducted by adding different concentrations of Cu^{2+} and the synthesized ratiometric probes into a spectrophotometer quartz cuvette to make the concentration gradient of Cu^{2+} range from 0 μM to 30.0 μM. The visual color changes were observed under a UV lamp. The fluorescence spectra were collected right after each addition due to the high sensitivity of the nanosensors to Cu^{2+}.

Selectivity and Interference Tests. To assess the selectivity of the dual-emission NPs to Cu^{2+}, the ratio of the F_{650}/F_{425} fluorescence intensity of the nanosensor exposed to other metal ions, such as Al^{3+}, Fe^{3+}, Sn^{2+}, Pb^{2+}, Ca^{2+}, Hg^{2+}, Zn^{2+}, Cd^{2+}, Mn^{2+}, and Ag^{+} was studied under the same conditions. A volume of 50 μL of the selected metal ions with the concentration of 60 μM was added into 250 μL of the as-synthesized ratiometric nanoprobes to reach the final concentration of 10 μM, respectively. Afterward, the mixtures were added to a spectrophotometer quartz cuvette ready for fluorescence spectra recording. Afterward, a certain concentration of Cu^{2+}, which was prepared in advance, was added directly to the nanocomposite mixtures, and the fluorescence spectra were recorded once more.

MTT Assay and Intracellular Fluorescence Imaging. HeLa cells (provided by professor Han's laboratory) were incubated in culture bottles and grown in DMEM with the addition of 10% FBS and 1% penicillin/streptomycin at 37 °C in 5% CO_2 atmosphere for 24 h. Different concentrations of the as-prepared dual-emission NPs were added for further incubation for 24 h. Then, 100 μL of the new culture medium containing MTT (10 μL, 5 mg/mL) was then added, followed by incubating for 4 h to allow the formation of formazan dye. The absorbance optical density of the purple formazan at 490 nm was measured on the enzyme-linked immunosorbent detector.

We sought to assess whether the nanosensor could report changes by ratiometric fluorescence imaging when cells were treated with exogenous Cu^{2+} sources. One day before imaging, HeLa cells were cultured in DMEM supplemented with 10% fetal bovine serum (FBS, Hyclone) for 24 h, to make cells

DOI: 10.1021/acs.analchem.6b01941
Anal. Chem. 2016, 88, 7395−7403

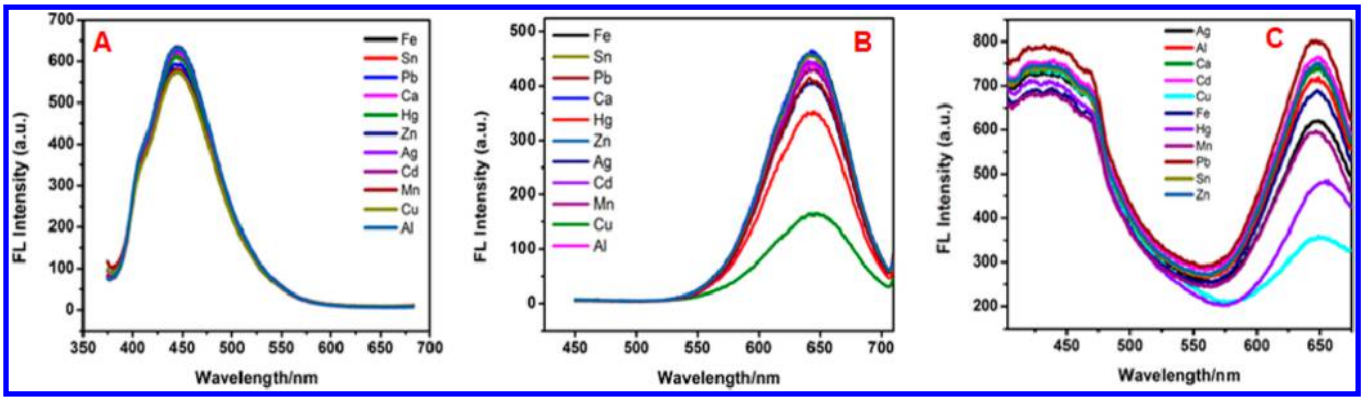

Figure 1. Fluorescence response of CDs-APTS (A), QDs (B), and CDs@QDs@SiO_2 (C) to 10 μM of different metal ions.

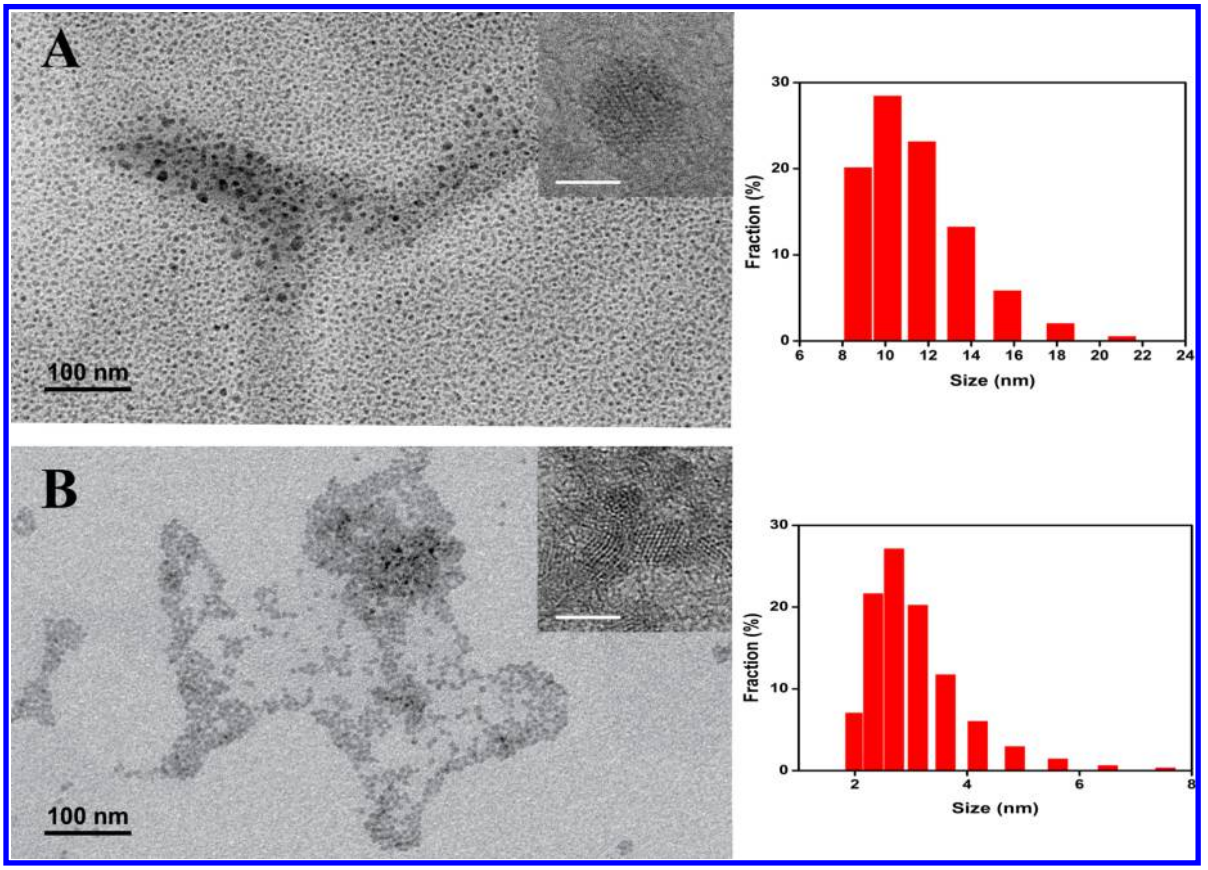

Figure 2. TEM images of (A) CDs, (B) QDs, and corresponding size distributions (inset, corresponding HRTEM images of CDs and QDs; scale bar, 5 nm).

stretched and plated onto the 18 mm coverslips. Then, 5 μM of $CuCl_2$ was prepared using DMEM in advance and added directly to the media of the cell 3 h prior to imaging, and named as group A. In contrast, another group B was cultured without 5 μM of $CuCl_2$ in the media. Afterward, we added 1.6 mg/mL nanosensor into group A−B, respectively, and incubated for another 12 h. The excess nanosensor was removed and each well was washed 3−4 times with PBS to make sure there is no any fluorescence nanosensor floating on the surface. Confocal fluorescent images were obtained with a Zeiss 510 META confocal laser scanning microscope, and the dual-emission silica NPs fluorescent intensity was excited and collected through the blue channel and the red channel, respectively.

RESULTS AND DISCUSSION

Characteristics of the CDs-Coated and QDs-Loaded Silica NPs. In this work, (3-aminopropyl) triethoxysilane (APTS) was selected for the preparation of CDs (CDs-APTS) that contained multiple amino groups. CDs-APTS were used as the reference signal because their fluorescence spectra showed no significant changes after the addition of Cu^{2+} as well as other metal ions (Figure 1A). In contrast, the fluorescence of the MPA-capped QDs was severely quenched by adding metal ions, particularly by the addition of Cu^{2+}. Therefore, MPA-capped QDs were chosen as the response signal (Figure 1B).

The high-resolution TEM images in Figure 2 showed that the mean diameters of the as-prepared QDs and CDs were ~4.5 ± 0.5 nm and ~9 ± 0.5 nm, and the corresponding

DOI: 10.1021/acs.analchem.6b01941
Anal. Chem. 2016, 88, 7395−7403

dynamic light scattering (DLS) measurements showed that the mean diameters of QDs and CDs were 3.8 ± 0.5 nm and 9.5 ± 0.5 nm, respectively. As displayed in the HRTEM images (Figure 3), the diameter size of the bare silica NPs was

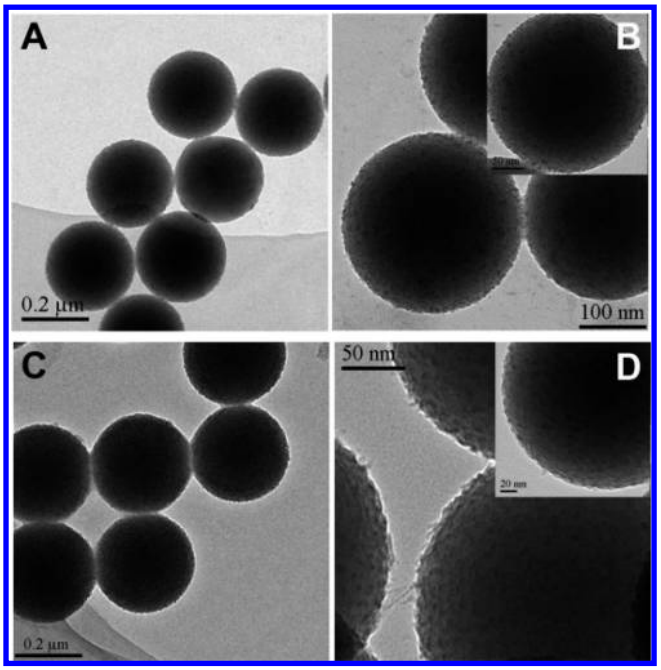

Figure 3. HRTEM of QDs@SiO_2 (A,B) and CDs@QDs@SiO_2 (C,D).

approximately 250 nm, while it was increased by 10 and 5 nm with the addition of QDs and CDs, respectively, and finally reaching 265 nm. The activated QDs were covalently linked through the reaction between amino and carboxyl groups on the surface of SiO_2 NPs to form QDs-loaded silica hybrid spheres, whose aqueous solution exhibited a robust red emission similarly to the primary QDs when excited by a UV lamp. The QDs-loaded silica hybrid spheres were then coated with CDs, resulting in a gel-like surface as shown in Figure 3C,D. All of the above can conclude the successful loading of QDs and coating the surface of the silica NPs with CDs. Additionally, the zeta potentials of the bare silica NPs, the functionalized amino-silica NPs, QDs-loaded silica NPs, the final CDs-coated, and QDs-loaded dual-emission silica NPs are −36.1 mV, 29.4 mV, −25.7 mV, and 30.3 mV, respectively (Figure S1).

To obtain the optimal excitation wavelength for the dual-emission nanosensors, we recorded the fluorescence spectra at different excitation wavelengths. Along with the increase of excitation wavelength, the blue emission intensity of CDs was observed to decrease significantly, and that of QDs also decreased. More importantly, when excited at 350 nm, the CDs as the reference signal of our probe exhibited the strongest fluorescence emission (Figure S2). As observed in (Figure 4) that the wavelength difference in the strong emission peak is as large as 225 nm between CDs and QDs (425 and 650 nm), respectively, which can effectively exclude the interference among the two emission peaks, and is favorable for the NPs to act as ratiometric fluorescence nanoprobe for the recognition of metal ions. Also, the quantum dots as signal labels loaded on the surface of silica microspheres, instead of traditionally embedded in the silica microspheres, can maintain the

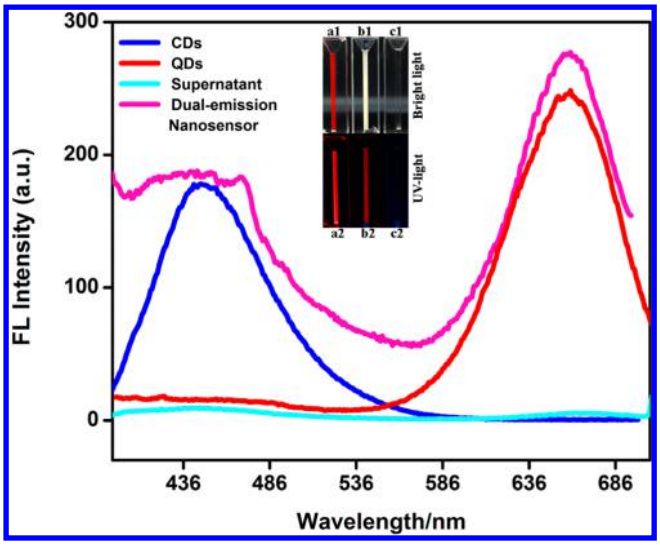

Figure 4. Fluorescence spectra of CDs (blue), QDs (red), dual-emission silica NPs nanosensors (pink), and the supernatant of the dual-emission silica NPs (green). The photos of QDs (a1), dual-emission silica NPs (b1), CDs (c1) under the bright light and the photos of QDs (a2), dual-emission silica NPs (b2), CDs (c2) under the UV light.

brightness and stability of the fluorescence signal as shown in the picture inserted in Figure 4.

The XPS spectra and elemental compositions of the QDs-loaded silica NPs and the final CDs-coated and QDs-loaded nanosensors were also obtained and analyzed to verify the loading of CDs on the surface of QDs-loaded silica NPs. The results displayed that only the carbon element content was increased, and the contents of oxygen, silicon, and cadmium were all decreased after the loading of CDs on the surface of the QDs-loaded silica NPs (Figure 5). These results are in accordance with those of the energy dispersive X-ray (EDX) analysis (Figure S3).

Selectivity of CDs-Coated and QDs-Loaded Silica NPs as a Ratiometric Nanoprobe for Detecting Metal Ions. The specific selectivity of CDs-coated and QDs-loaded silica NPs to the target metal ions over other metal ions is essential for a probe when applied in environmental systems; particularly, it is more challenging to the complicated intracellular system. As shown in (Figure 6), besides the effect of Cu^{2+}, the impact of other cations (Al^{3+}, Fe^{3+}, Sn^{2+}, Pb^{2+}, Ca^{2+}, Hg^{2+}, Zn^{2+}, Cd^{2+}, Mn^{2+}, Cu^{2+}, and Ag^{+}) on the changes of the fluorescence ratio were studied under the same conditions. After the addition of 10 μM of Al^{3+}, Fe^{3+}, Sn^{2+}, Pb^{2+}, Ca^{2+}, Hg^{2+}, Zn^{2+}, Cd^{2+}, Mn^{2+}, Cu^{2+}, and Ag^{+} to an equal concentration of the fluorescent probe, only Cu^{2+} could severely quench the fluorescence of QDs to make an 80% decrease of the intensity of F_{650}/F_{425}. In contrast, other metal ions have no significant quenching effect on QDs fluorescent intensity. While with subsequent addition of Cu^{2+} to all of the above solutions containing other metal ions, the F_{650}/F_{425} ratio was decreased obviously and made the final intensity of F_{650}/F_{425} less than 20%, indicating that the coexistence of these metal ions has minor interloping on the good selectivity of the dual-emission NPs when exposed to copper ions.

Detection Limit of Cu^{2+}. As shown in Figure 7, when the concentration of Cu^{2+} increased, the fluorescence color changed continuously from red to blue along with the variations in the intensity ratio of both two fluorescence

DOI: 10.1021/acs.analchem.6b01941
Anal. Chem. 2016, 88, 7395−7403

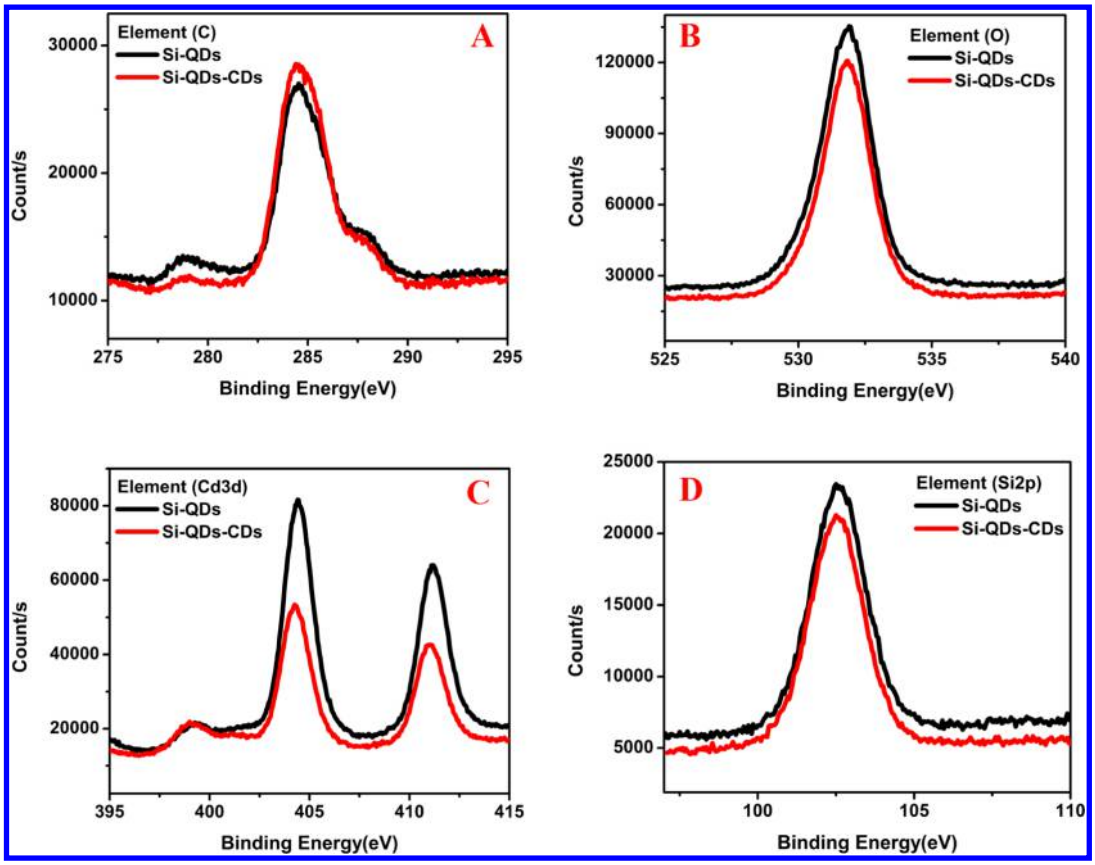

Figure 5. XPS results of C (A), O (B), Cd (C), and Si (D) elements of QDs@SiO_2 (black) and CDs@QDs@SiO_2 (red).

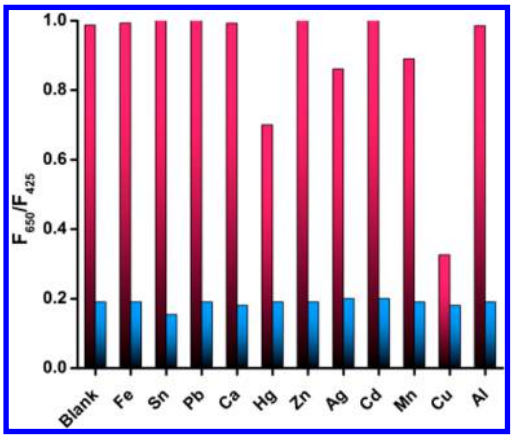

Figure 6. Plots of F_{650}/F_{425} ratio fluorescence intensity dual emission NPs in the absence of various metal ions (10 μM, red bars) and the following addition of Cu^{2+} (10 μM, blue bars).

emission peaks, which may possibly be visibly observed by the naked eye. Besides, the F_{650}/F_{425} ratio decreased considerably. The red fluorescence at 650 nm decreased considerably followed by the increase of Cu^{2+} at the concentration ranging from 0 to 30 μM. While the main concentration of Cu^{2+} was greater than 30 μM, the fluorescence of QDs was entirely quenched and the dual-emission NPs fluorescence spectra no more showed any change through the increase of Cu^{2+}. A good linearity between the F_{650}/F_{425} ratio and Cu^{2+} concentration was obtained when the Cu^{2+}concentration ranged from 0 to 30 μM (Figure 7, inset), and the limit of detection (signal-to-noise ratio of S/N = 3) was estimated to be 140 nM, compared to the supreme concentration (1.3 ppm, about 20 μM) of Cu^{2+} legalized by the U.S. Environment Protection Agency in drinking water.

Effect of pH on the Fluorescence Intensity of CDs-Coated and QDs-Loaded Silica. NPs. In addition, we also investigated the influence of pH on the fluorescent intensity of the dual-emission nanosensor. The fluorescent intensity showed no significant changes at pH ranging from 5 to 11 but was reduced at pH below 5.0 and greater than 11.0 (Figure 8A), suggesting that our dual-emission nanosensor can be applied in biological imaging and in many environmental applications due to its high biocompatibility. Meanwhile, we preformed the stability test of the nanohybrid composite in the pH of 7.4 over a period of 36 days and showed good fluorescent intensity as well.

Imaging of Cu^{2+} in HeLa Cells. HeLa cells were chosen to investigate the viability of the dual-emission NPs for intracellular Cu^{2+} imaging, by incubating with dual-emission nanosensors. As shown in Figure 8B, the viability of HeLa cells was found to be quite high at the concentration of SiO_2@QDs@CDs as high as 1.6 mg/mL after up to 24 h exposure. Furthermore, the ratiometric confocal fluorescence cellular imaging experiment for intracellular Cu^{2+} was performed. The double channel fluorescence images were captured by a 405 nm laser with a laser-scanning confocal microscope in blue and red channels with excitation as shown in (Figure 9). We can observe the difference between the untreated and the treated with exogenous Cu^{2+} in HeLa cells as follows: (1) incubated HeLa cells with dual-emission nanosensors (1.6 mg/mL) at room temperature showed clearly red intracellular fluorescence, because the dark blue intracellular fluorescence is almost obscured by the twinkling red fluorescence (Figure 9A1, B1). (2) After the addition of Cu^{2+} to the HeLa cells, the probe was

DOI: 10.1021/acs.analchem.6b01941
Anal. Chem. 2016, 88, 7395−7403

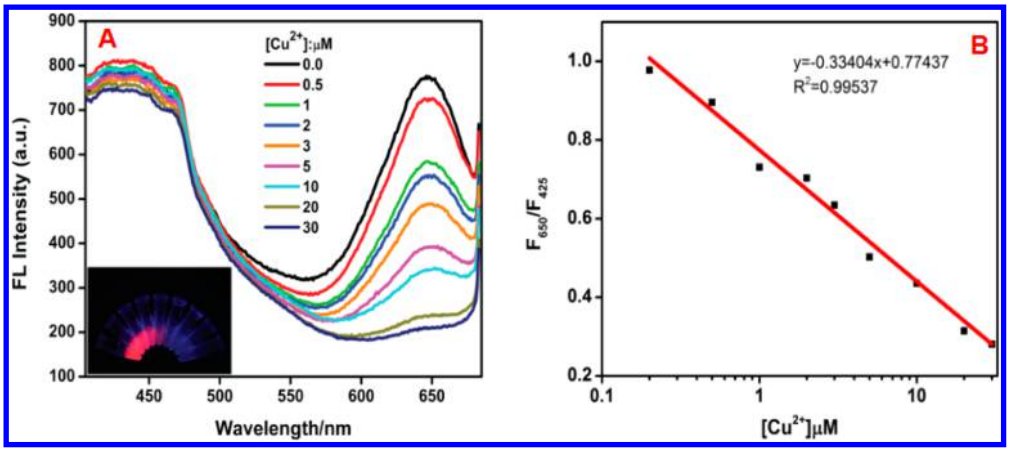

Figure 7. (A) Fluorescence spectra change of SiO_2@QDs@CDs in the presence of various concentrations of Cu^{2+}. The concentration of Cu^{2+} from top to bottom: 0, 0.5, 1, 2, 3, 5, 10, 20, and 30 μM, respectively, and the color changes from red to blue under the UV light was inserted. (B) Linear relationship between the fluorescence intensity of F_{650}/F_{425} of SiO_2@QDs@CDs and the concentration of Cu^{2+}.

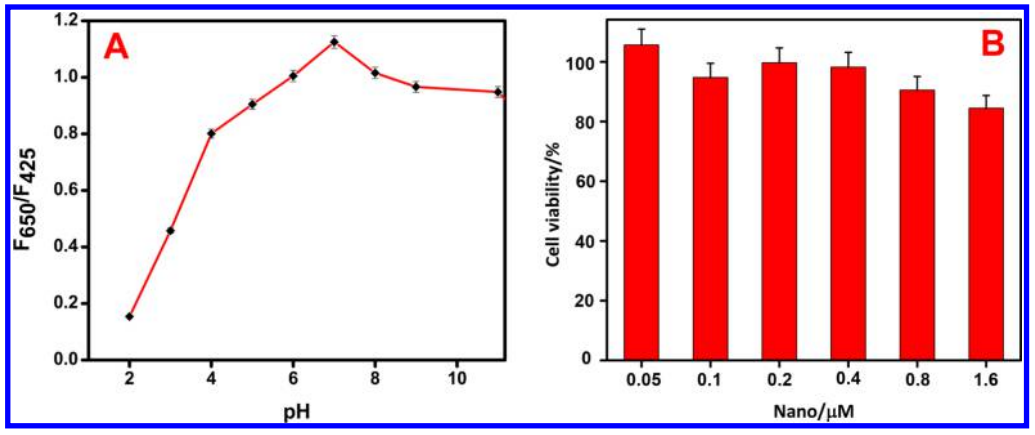

Figure 8. Effect of pH on the fluorescence intensity ratio (F_{650}/F_{425}) of the dual-emission NPs (A), and the cell viability of HeLa cells after 24 h treatment with nanosensors calculated from the MTT assay (B).

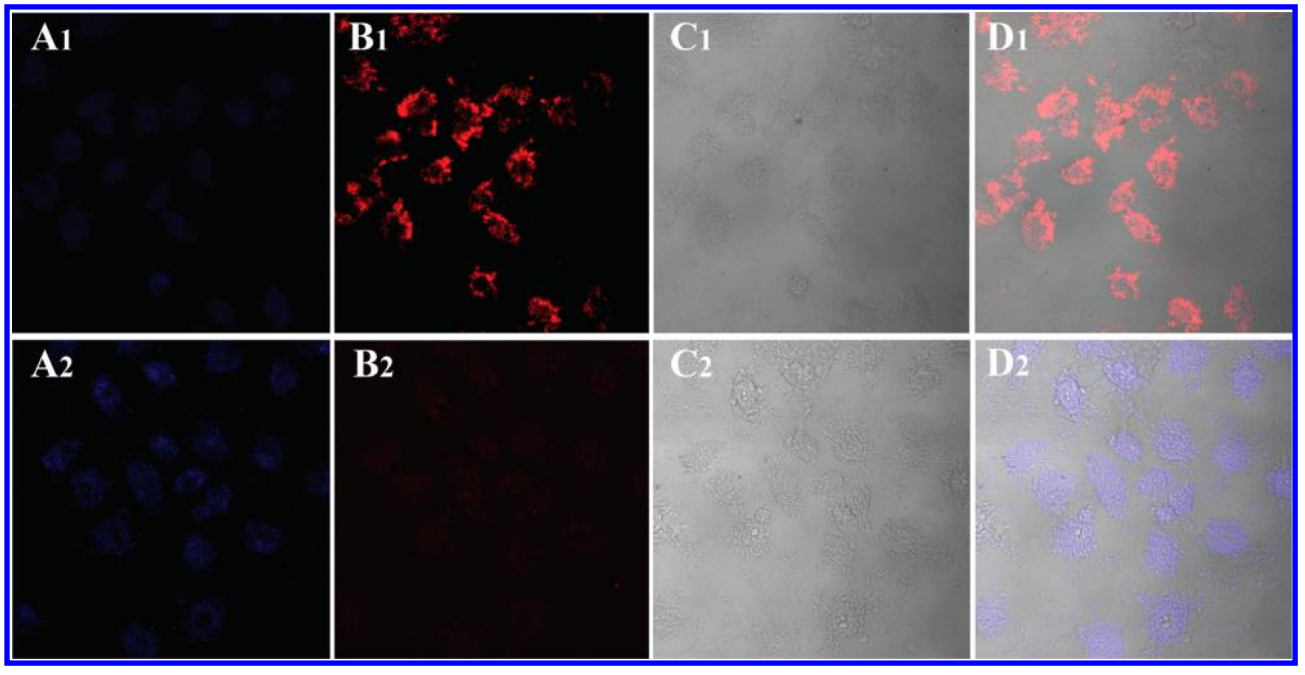

Figure 9. Confocal fluorescence images of HeLa cells before (A1, B1, C1, D1) and after (A2, B2, C2, D2) addition of Cu^{2+} (10 μM). (A1, A2) Blue channel fluorescence images, (B1, B2) red channel fluorescence images, (D1, D2) overlay of bright field and fluorescence images (C1, C2). Scale bar: 20 μm.

DOI: 10.1021/acs.analchem.6b01941
Anal. Chem. 2016, 88, 7395−7403

potent for specific recognition of Cu^{2+} in cells and the blue color became clearer along with the quenching of red fluorescence, which is identical to the results of the analysis of the fluorescence intensity of the dual-emission NPs to Cu^{2+} in PB buffer solution (Figure 9A2, B2). The sufficient cellular uptake of the dual-emission nanosensor demonstrates that our method can be further expanded to ratiometric intracellular imaging for more complex biological samples.

CONCLUSION

In conclusion, a ratiometric fluorescence nanohybrid composite for Cu^{2+} was designed and prepared by coating the as-prepared QDs-loaded silica NPs with CDs on the outer surface via a carbodiimide-mediated approach. Under the exposure to Cu^{2+}, only QDs can be quenched, which leads to the ratiometric fluorescence response to Cu^{2+} in aqueous solution. In this core−satellite hybrid nanosensor, the brightness and stability of the fluorescence signal were enhanced by using silica microspheres as a carrier loaded with a large number of quantum dots as signal labels on the surface. Meanwhile, the toxicity of the nanosensor was tremendously reduced by densely packed carbon dots around the SiO_2@QDs nanomicrospheres. The results of the assay of metal ion selectivity have revealed that this ratiometric fluorescence nanosensor has lowered the threshold for detecting Cu^{2+} and thus improved the sensibility. Furthermore, this ratiometric nanosensor was efficaciously applied for the ratiometric intracellular imaging of Cu^{2+} in HeLa cells, which validates its efficiency on-site visual determination of Cu^{2+} in biological applications.

ASSOCIATED CONTENT

Supporting Information

The Supporting Information is available free of charge on the ACS Publications website at DOI: 10.1021/acs.analchem.6b01941.

Zeta potentials of the bared silica NPs, functionalized amino-silica NPs, QDs-loaded silica NPs, and final CDs-coated and QDs-loaded dual-emission silica NPs; fluorescence spectra of the dual-emission NPs; EDX analysis of the dual-emission NPs from aluminum plate; intensity of F_{650}/F_{425} influenced by twice the concentration of copper ion and other metal ions; cell viabilities of HeLa cells calculated from MTT assay after 24 h treatment with nanosensors before and after coated with CDs and with QDs and CDs; and FT-IR spectra of the synthesized nanosensor, CDs, and QDs (PDF)

AUTHOR INFORMATION

Corresponding Author

*Phone: +86-27-87288505. Fax: +86-27-87288505. E-mail: hyhan@mail.hzau.edu.cn.

Notes

The authors declare no competing financial interest.

ACKNOWLEDGMENTS

We gratefully acknowledge the financial support from National Natural Science Foundation of China (Grants 21375043 and 21175051).

REFERENCES

(1) Ghrefat, H.; Yusuf, N. *Chemosphere* **2006**, *65*, 2114−2121.
(2) Gaetke, L. *Toxicology* **2003**, *189*, 147−163.
(3) Emerit, J.; Edeas, M.; Bricaire, F. *Biomed. Pharmacother.* **2004**, *58*, 39−46.
(4) Viles, J. H. *Coord. Chem. Rev.* **2012**, *256*, 2271−2284.
(5) Zietz, B. P.; Dassel de Vergara, J.; Dunkelberg, H. *Environ. Res.* **2003**, *92*, 129−138.
(6) Zietz, B. P.; Dieter, H. H.; Lakomek, M.; Schneider, H.; KeßlerGaedtke, B.; Dunkelberg, H. *Sci. Total Environ.* **2003**, *302*, 127−144.
(7) Formica, M.; Fusi, V.; Giorgi, L.; Micheloni, M. *Coord. Chem. Rev.* **2012**, *256*, 170−192.
(8) Jeong, Y.; Yoon, J. *Inorg. Chim. Acta* **2012**, *381*, 2−14.
(9) Doussineau, T.; Schulz, A.; Lapresta-Fernandez, A.; Moro, A.; Korsten, S.; Trupp, S.; Mohr, G. J. *Chem. - Eur. J.* **2010**, *16*, 10290−10299.
(10) Wang, Y. Q.; Zhao, T.; He, X. W.; Li, W. Y.; Zhang, Y. K. *Biosens. Bioelectron.* **2014**, *51*, 40−46.
(11) Yan, X.; Li, H.; Li, Y.; Su, X. *Anal. Chim. Acta* **2014**, *852*, 189−195.
(12) Li, P.; Xie, T.; Fan, N.; Li, K.; Tang, B. *Chem. Commun.* **2012**, *48*, 2077−2079.
(13) Wu, C.; Bull, B.; Christensen, K.; McNeill, J. *Angew. Chem., Int. Ed.* **2009**, *48*, 2741−2745.
(14) Barman, S.; Sadhukhan, M. *J. Mater. Chem.* **2012**, *22*, 21832−21837.
(15) Adhikari, S.; Ghosh, A.; Sahana, A.; Guria, S.; Das, D. *Anal. Chem.* **2016**, *88*, 1106−1110.
(16) Zhou, L.; Wang, Q.; Zhang, X. B.; Tan, W. *Anal. Chem.* **2015**, *87*, 4503−4507.
(17) Zhu, X.; Zhao, T.; Nie, Z.; Liu, Y.; Yao, S. *Anal. Chem.* **2015**, *87*, 8524−8530.
(18) Zhang, G.; Sun, Y.; He, X.; Zhang, W.; Tian, M.; Feng, R.; Zhang, R.; Li, X.; Guo, L.; Yu, X.; Zhang, S. *Anal. Chem.* **2015**, *87*, 12088−12095.
(19) Zhao, M.; Fan, G. C.; Chen, J. J.; Shi, J. J.; Zhu, J. J. *Anal. Chem.* **2015**, *87*, 12340−12347.
(20) Liu, Y.; Ye, M.; Ge, Q.; Qu, X.; Guo, Q.; Hu, X.; Sun, Q. *Anal. Chem.* **2016**, *88*, 1768−1774.
(21) Wu, X.; Li, L.; Shi, W.; Gong, Q.; Li, X.; Ma, H. *Anal. Chem.* **2016**, *88*, 1440−1446.
(22) Cao, B.; Yuan, C.; Liu, B.; Jiang, C.; Guan, G.; Han, M. *Anal. Chim. Acta* **2013**, *786*, 146−152.
(23) Wang, K.; Qian, J.; Jiang, D.; Yang, Z.; Du, X.; Wang, K. *Biosens. Bioelectron.* **2015**, *65*, 83−90.
(24) Yao, J.; Zhang, K.; Zhu, H.; Ma, F.; Sun, M.; Yu, H.; Sun, J.; Wang, S. *Anal. Chem.* **2013**, *85*, 6461−6468.
(25) Yan, X.; Li, H.; Han, X.; Su, X. *Biosens. Bioelectron.* **2015**, *74*, 277−283.
(26) Sun, X.; Liu, P.; Wu, L.; Liu, B. *Analyst* **2015**, *140*, 6742−6747.
(27) Zhu, S.; Meng, Q.; Wang, L.; Zhang, J.; Song, Y.; Jin, H.; Zhang, K.; Sun, H.; Wang, H.; Yang, B. *Angew. Chem., Int. Ed.* **2013**, *52*, 3953−3957.
(28) Li, H.; He, X.; Kang, Z.; Huang, H.; Liu, Y.; Liu, J.; Lian, S.; Tsang, C. H.; Yang, X.; Lee, S. T. *Angew. Chem., Int. Ed.* **2010**, *49*, 4430−4434.
(29) Tan, M.; Zhang, L.; Tang, R.; Song, X.; Li, Y.; Wu, H.; Wang, Y.; Lv, G.; Liu, W.; Ma, X. *Talanta* **2013**, *115*, 950−956.
(30) Huang, Y. F.; Zhou, X.; Zhou, R.; Zhang, H.; Kang, K. B.; Zhao, M.; Peng, Y.; Wang, Q.; Zhang, H. L.; Qiu, W. Y. *Chem. - Eur. J.* **2014**, *20*, 5640−5648.
(31) Liu, Y.; Liu, L.; He, Y.; Zhu, L.; Ma, H. *Anal. Chem.* **2015**, *87*, 5286−5293.
(32) Zhou, J.; Yang, Y.; Zhang, C. Y. *Chem. Rev.* **2015**, *115*, 11669−11717.
(33) Vaidya, S. V.; Couzis, A.; Maldarelli, C. *Langmuir* **2015**, *31*, 3167−3179.
(34) Foda, M. F.; Huang, L.; Shao, F.; Han, H. Y. *ACS Appl. Mater. Interfaces* **2014**, *6*, 2011−2017.
(35) Wu, P.; Zhao, T.; Wang, S.; Hou, X. *Nanoscale* **2014**, *6*, 43−64.
(36) Chen, Y.; Rosenzweig, Z. *Anal. Chem.* **2002**, *74*, 5132−5138.

DOI: 10.1021/acs.analchem.6b01941
Anal. Chem. 2016, 88, 7395−7403

(37) Xie, H. Y.; Liang, J. G.; Zhang, Z. L.; Liu, Y.; He, Z. K.; Pang, D. W. *Spectrochim. Acta, Part A* **2004**, *60*, 2527−2530.
(38) Fernández-Argüelles, M. T.; Jin, W. J.; Costa-Fernández, J. M.; Pereiro, R.; Sanz-Medel, A. *Anal. Chim. Acta* **2005**, *549*, 20−25.
(39) Gattás-Asfura, K. M.; Leblanc, R. M. *Chem. Commun.* **2003**, 2684.
(40) Son, D. H.; Hughes, S. M.; Yin, Y.; Alivisatos, A. P. *Science* **2004**, *306*, 1009−1012.
(41) Liu, X.; Zhang, N.; Bing, T.; Shangguan, D. *Anal. Chem.* **2014**, *86*, 2289−2296.
(42) Zhang, Y.; Li, Y.; Yan, X. P. *Small* **2009**, *5*, 185−189.
(43) Seo, H.; Kim, S. W. *Chem. Mater.* **2007**, *19*, 2715−2717.
(44) Zeng, Q.; Kong, X.; Sun, Y.; Zhang, Y.; Tu, L.; Zhao, J.; Zhang, H. *J. Phys. Chem. C* **2008**, *112*, 8587−8593.
(45) Smith, A. M.; Nie, S. *Acc. Chem. Res.* **2010**, *43*, 190−200.
(46) Wang, J.; Li, N.; Shao, F.; Han, H. *Sens. Actuators, B* **2015**, *207*, 74−82.
(47) Stöber, W.; Fink, A.; Bohn, E. *J. Colloid Interface Sci.* **1968**, *26*, 62−69.
(48) Wu, L.; Li, X.; Shao, K.; Ye, S.; Liu, C.; Zhang, C.; Han, H. *Anal. Chim. Acta* **2015**, *887*, 192−200.

DOI: 10.1021/acs.analchem.6b01941
Anal. Chem. 2016, 88, 7395−7403